Airborne Remote Sensing Used to Estimate Percent Canopy Cover and to Extract Canopy Temperature from Scene Temperature in Cotton

W. R. DeTar, J. V. Penner

Abstract. *The goal of this research was to separate the soil and plant temperatures and create an image map of plant water stress. Data from hyperspectral imagery (HSI) and thermal infrared (TIR) sensors were collected using an airborne platform over three seasons, involving three different varieties of Acala cotton, four different fields, and a total of ten flights. The first step was to measure the percent canopy cover, which ranged from 30% to 100%. Using linear multiple regression, percent canopy cover, measured manually in the field, was found to be closely related to several new vegetation indices, taken from among 60 narrow bands in the wavelength range of 429 to 1010 nm. The highest coefficient of determination (r^2) for a three-parameter hyperspectral model was 0.931, and it included the wavelengths 676, 753, and 773 nm. A two-parameter model using 676 and 966 nm worked especially well. A weighted version of the normalized difference vegetation index (NDVI) was found to relate well to percent canopy cover, but not quite as well as some non-normalized band combinations. Using the two-parameter model, the percent canopy cover was calculated for every part of two experimental fields that had originally been set up to compare the yields from water-stressed versus unstressed treatments. The mean value for scene temperature for each plot was plotted against the mean value of percent canopy cover for each plot. Using analysis of covariance, the scene temperatures were projected to what they would be at 100% canopy. The procedure showed that the canopy for the water-stressed treatment had a significantly higher temperature than the unstressed control, which means that it was indeed stressed. Using analysis of covariance, the green-red difference was found to be an indicator of both percent canopy cover and plant water stress. An image map was produced showing the canopy temperature at every pixel in the field, with a spatial resolution of about 1.0 m. The main finding was that the plant water stress in Acala cotton could be detected with airborne remote sensing under the conditions of partial canopy over a dry soil surface. These results should be useful in selecting filters for multispectral cameras and for selecting the wavebands for HSI sensors when attempting to measure degree of vegetative cover. A straightforward method is presented for separating canopy temperature from soil temperature, and a procedure is given for producing a detailed map of canopy temperature in the field.*

Keywords. *Analysis of covariance, Band selection, Multiple regression, Plant water stress, Vegetation indices.*

Due to the spatial and temporal variability of growth-related crop characteristics, in-field measurements at the number of discrete points necessary to provide accuracy and confidence are often cost prohibitive. Remote sensing can provide the spatial distribution necessary with image maps showing properties of every part of every field (Maas, 1998; Moran et al., 1997; Dawson, 1997). Crop yield can be greatly affected by plant water stress. However, it is important to apply stress-relieving irrigation water in a judicious manner to avoid environmental problems and to keep the cost down on a limited and expensive resource. The development of the infrared thermometer made it possible to measure canopy temperature without physically touching the plant (Ehrler at al., 1978), and the temperature of the plant canopy can be a measure of plant water stress. Many different types of vegetation indices have been used to empirically relate remotely sensed data to crop properties (Thenkabail et al., 2000; Thorp et al., 2004). Moran et al. (1989) showed that water stress on alfalfa caused a reduction in the spectral reflectance in both the near-infrared (NIR) and red regions. Jackson et al. (1983) used various combinations of bands, and concluded that water stress on wheat could not be detected until there was a stress-induced retardation in growth.

The relationship between water stress and canopy temperature for cotton and corn was studied by Wanjura and Upchurch (2000). Jackson et al. (1981) discussed the crop water stress index (CWSI) and the no-stress baseline in their work with canopy temperature as a measure of stress. Clarke (1997) used the water deficit index (WDI) from Moran et al. (1994) to show temperature rise and stress in melons under partial canopy. They noted that there was no precise remotely sensed equivalent to percent canopy cover. Goel et al. (2003) used multiple regression to select narrow bands from hyperspectral imagery (HSI) data to predict several biophysical properties of corn, but did not include percent canopy cover. Bajwa et al. (2004) used principal component analysis and artificial neural network based models to select the best 20

Submitted for review in May 2006 as manuscript number SW 6469; approved for publication by the Soil & Water Division of ASABE in January 2007.

The authors are **William R. DeTar, ASABE Member Engineer,** Research Agricultural Engineer, and **John V. Penner,** Engineering Technician, USDA-ARS Western Integrated Cropping Systems Research, Shafter, California. **Corresponding author:** Dr. William R. DeTar, USDA-ARS, 17053 N. Shafter Ave., Shafter, CA 93263; phone: 661-746-8011; fax: 661-746-1619; e-mail: wrdetar@pw.ars.usda.gov.

bands for soybean canopy cover. The effect of developing moisture stress was shown by Maas et al. (1999) to be a rise in canopy temperature. They used airborne thermal infrared (TIR) data from daily flights over drip-irrigated cotton plots suddenly deprived of water. Temperatures in the stressed plots rose by as much as 10°C above those in unstressed plots.

The primary goal of this study was to use airborne hyperspectral and TIR data to provide detailed images of plant water stress in cotton fields under partial canopy. Under partial canopy conditions, however, the high temperature of the exposed soil can have an overwhelming influence over the average (scene) temperature. The first step was to get a measure of the degree of crop canopy cover, and then separate the canopy temperature from the soil temperature.

Materials and Methods

Experimental Fields

The site for this study was the Shafter Research and Extension Center of the University of California, which is located near the southern end of the San Joaquin Valley, at 35° 31′ N, 119° 17′ W, and 109 m above sea level. Annual average precipitation is 167 mm, with little rainfall from May to September. All the soils on the station are mapped as a Wasco sandy loam (coarse-loamy, mixed, non-acid, thermic Typic Torriothents). In 2001, Acala NemX cotton was grown in field 42, which is a 2.6 ha field, 85 m wide × 302 m long (fig. 1). Plant rows were 0.76 m apart and ran the length of the field, which is in the east-west direction. Irrigation was done with a subsurface drip system, with a dripper line buried 0.26 m below grade in every plant row and running the full length of the field. Water was applied on a daily basis. The field was divided into four narrow strips, each 21.3 m wide. Each of these strip plots was on a separate irrigation circuit, and they were labeled A, B, C, and D from south to north. Plots B and D were irrigated normally, applying the average ET required (see DeTar, 2004) based on a system efficiency of 90%.

In order to simulate a furrow- or sprinkler-irrigated heavier soil where an irrigation would be required about once every four weeks, the A and C plots were deficit-irrigated by about 25% starting 25 June 2001, applying an average of 1.9 mm d^{-1} less than the depth normally required. The average moisture available in the root zone was about 127 mm at field capacity. Allen et al. (1998) gave the threshold point for start of water stress as 56% depletion when the normal crop ET is 7.1 mm d^{-1}. The plan was to reach this point at 127*0.56/1.9 = 37 days after initiation, which would be 1 August.

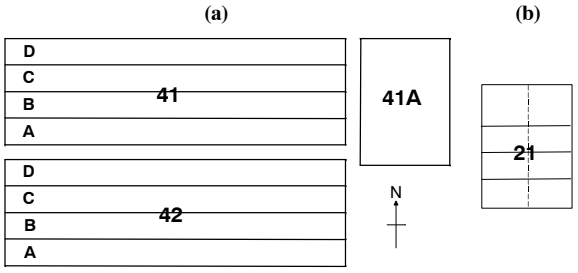

Figure 1. Plot plan of the four fields in the study: (a) orientation and relative location of three of the fields studied, and (b) field 21, which is located in a separate area approximately 1 km north of (a).

In 2002, field 42 and an adjacent field, field 41, were both planted to Acala PhytoGen-72 cotton. Field 41 had the same dimensions, layout, and irrigation system as field 42, but for 2002, the B and D plots were deficit-irrigated starting on 27 June 2002, and the A and C plots were irrigated normally.

In 2003, field 21, a 0.97 ha plot with a somewhat finer-textured soil than most of the Research Center, was planted to Acala Maxxa cotton. The field dimensions were 87 × 110 m, with 1.0 m spacing between the plant rows, which ran in the east-west direction. There were 12 buffer rows on the north side of the field, the direction of prevailing winds, and four buffer rows on the south side. The remaining area was divided into 16 plots, separated by 2 m wide walkways, with each plot measuring 21 × 22 m. Half the plots were water stressed; half were unstressed. The field was furrow-irrigated normally on two-week intervals, with about 115 mm being applied each irrigation. To ensure significant water stress at the time of a flight, two weeks before the flight, the stressed plots were given only half the normal depth of water. Leaf water potential (Hake et al., 1996) was measured before the flights, using two leaves from each of the eight main plots.

For 2002 and 2003, field 41A, a 0.7 ha plot, was set up to determine the optimum level of water application to Acala Maxxa and Acala PhytoGen-72 cotton, using six different application rates. This field has the same coarse-textured soil as in fields 41 and 42. It also had the same row spacing, but the rows ran in the north-south direction. The irrigation system was subsurface drip. Application rates for the treatments ranged from 33% of normal to 144% of normal. The surface of the soil was dry in all four fields at the time of the flights.

Equipment and Ground Truthing for Flights

Over the three years of tests, ten data acquisition flights were made during the period before full canopy was reached. Flight dates and times are given in table 1. The light airplane (Cessna 206/210), pilot, camera operator, and pre-processing were all provided by Opto-Knowledge Systems, Inc. (OKSI) of Torrance, California. OKSI also provided a hyperspectral (HSI) camera, called the Airborne Visible-Near-Infrared (AVNIR) system, which had a spatial resolution of 0.8 m from an altitude of 1500 m, with 60 bands of reflectance data in the range of 429 to 1010 nm and a spectral resolution of 10 nm. Also included from all flights were data from a set of cameras provided by the USDA-ARS at Shafter called the Shafter Airborne Multispectral (MSI) Remote Sensing System (SAMRSS), developed by Maas et al. (1999). This package included three multispectral Dalsa digital cameras (Dalsa, Inc., Waterloo, Ont.), one for the green range of 545 to 555 nm, one for the red range of 675 to 685 nm, and one near-infrared (NIR) camera for the range 830 to 870 nm, all with a spatial resolution of 1 m. Also included in the package was a thermal infrared (TIR) camera (Indigo Merlin thermal imager from Indigo Systems, Santa Barbara, Cal.) with a range of 8000 to 14,000 nm and a spatial resolution of 2.4 m, and a video camera. Square white targets, 1.2 m on a side, were placed at the corners of every field for georeferencing.

On flight days, three 8 × 8 m fabric calibration panels (Tracor Aerospace, Inc., Austin, Texas) were spread out on the unpaved road at the east end of field 41. As near to flight time as possible, ground truthing was done with hand-held infrared thermometers, obtaining temperatures of unpaved

Table 1. Flight dates and times.

Flight No.	Flight Date	Flight Time (PST)[a]	Fields
1	20 June 2001	13:00[b]	42
2	5 July 2001	13:00[b]	42
3	11 July 2001	13:00[b]	42
4	18 June 2002	14:37	41, 42, 41A
5	25 June 2002	14:00	41, 42
6	1 July 2002	14:26	41, 42
7	8 July 2002	14:34	41, 42, 41A
8	9 July 2003	12:55	21, 41A
9	28 July 2003	14:44	21
10	20 August 2003	12:44	41A

[a] Solar noon is about 13:00 PDT.
[b] Approximate flight time.

roads, fallowed fields, smooth bare-soil walkways, stressed and unstressed canopies, calibration panels, a pond, unplanted but furrowed and cultivated soil at the east end of field 42, and nearby alfalfa fields. Air temperature and humidity (dry bulb and wet bulb) were measured above the canopy in the field and in areas around the field with a battery-aspirated psychrometer. Spectral radiometer readings of the calibration panels were taken in 2001 and 2002, using an LI-1800 spectroradiometer (Li-Cor, Inc., Lincoln, Neb.) and in 2003 they were taken with an ASD portable Vis/NIR reflectance spectrometer (Analytical Spectral Devices, Boulder, Colo.). All this data, along with data from the Research Center's weather station, was sent to OKSI within 3 h after the flight, to help with the pre-processing. Normal turnaround time for the processing was 24 h.

Data Analysis

Using ENVI, an image processing software (Research Systems, Inc., Boulder, Colo.), images of the individual fields were extracted from larger images acquired during the flights and exported as ASCII files for further processing. Excel was used to convert these files to a format useable by CoPlot v3.0 (CoHort Software, Monterey, Cal.) and by ArcView GIS v3.3 (ESRI, Redlands, Cal.). To extract detailed data for this part of the study, the HSI reflectance data for each field were loaded into ArcView, and a line tool was used to demarcate the boundary between irrigation treatments. Each of the irrigation plots in fields 41, 42, and 21 was then subdivided into smaller, equal-sized grid areas. The plots in field 41A were already rather small and were treated as grid areas. There were walkways in all fields, similar to the ones in field 21. Small areas of interest, measuring 4 × 4 m, were then established along the walkway, one in every grid area in fields 21 and 41A and in three test areas each in fields 41 and 42. For each flight date, the average fraction of canopy cover was estimated for each area of interest by measuring the width of the canopy with a meter stick and dividing by the row spacing, as reported by Maas (1998) and Wiegand et al. (1991). With the field data files still in ArcView, each of the areas of interest was selected using a select feature tool. The statistical average for the spectral response pattern was produced for each small area of interest. These data were entered into Excel with one area of interest to each row. Data from every flight were added to this file, and this area-of-interest file eventually grew to 300 rows of data, 60 columns wide. When the percent canopy cover (the dependent variable) was added into column 61, this file became the primary source for multiple regression analysis.

HSI data for the grid areas were also extracted and averaged in a manner similar to that for the small areas of interest, producing one line of averaged data for each grid area. Typical spectral response patterns were developed from this averaged grid-area file. Mean values of TIR scene temperatures for each grid area were also obtained for every flight using the select feature tool in ArcView.

Multiple Linear Regression

In order to find the combination of bands in the area-of-interest files that best correlated to the percent canopy cover, the files were imported into CoPlot, which accesses another program called CoStat to do the analysis. The percent canopy cover was considered the dependent variable, and the various band reflectances were the independent variables. An automatic procedure is available in which, after the number of bands to include in each multiple regression has been chosen, the program looks at every possible combination, returning only the r^2 values. The number of regressions required for pairs of bands out of 60 available is 60*59/(1*2) = 1770. To find the best three-band combinations required 60*59*58/(1*2*3) = 34,220 regressions. Four-band combinations required 487,635 regressions. The program automatically ranks and stores the results of the 100 best combinations (models).

The procedure above was also done for each individual flight. In looking at the best models for each flight, it was found to be nearly impossible to find a set of bands that worked consistently well on all flights. Occasionally, the same set of bands, from somewhere in the top 100 r^2 values of each flight, was found to work well in two or three flights, but even then the equations were dissimilar. It was felt that one way to find a consistent model for all the flights was to put all the data together in one file before regressing.

Multiple regression produces equations of the form:

$$G = a + b * X_1 + c * X_2 \quad (1)$$

where G is the percent canopy cover, and X_1 and X_2 are the reflectances for two bands in this two-parameter model. Equation 1 can also be written as:

$$G = a + b * (X_1 + m * X_2) \quad (2)$$

where $m = c/b$, and the expression in parentheses is a type of vegetation index, which can be expressed as:

$$I = X_1 + m * X_2 \quad (3)$$

Substituting equation 3 into equation 2 produces a simple linear equation:

$$G = a + b * I \quad (4)$$

A similar vegetation index was also developed for three- and four-parameter models.

Analysis of covariance was used in the last part of this work to separate the canopy temperature from the soil temperature. Analysis of covariance is a standard statistical procedure normally used to remove an effect in the field that is measured but not controlled. It creates a set of parallel regression lines, sometimes called a family of curves, through the data, and it allows the data to be adjusted to one level of the uncontrolled variable so that normal analysis of variance procedures can be applied.

Table 2. Bands with the 20 highest r^2 values for the equations relating percent canopy cover to wavelength, for one-, two-, three-, and four-parameter equations, using merged data from ten flights.

	One Parameter		Two Parameters		Three Parameters		Four Parameters	
Rank	Band (nm)	r^2	Bands (nm)	r^2	Bands (nm)	r^2	Bands (nm)	r^2
1	666	0.8023	763, 686	0.9192	773, 753, 676	0.9310	773, 753, 676, 531	0.9328
2	676	0.7947	966, 686	0.9189	773, 753, 686	0.9305	773, 753, 676, 521	0.9327
3	657	0.7888	966, 676	0.9187	773, 753, 657	0.9301	811, 773, 753, 676	0.9326
4	686	0.7731	763, 637	0.9186	928, 918, 676	0.9290	773, 753, 695, 686	0.9325
5	647	0.7583	870, 686	0.9185	773, 753, 647	0.9289	776, 753, 695, 676	0.9325
6	637	0.7553	860, 686	0.9184	928, 918, 686	0.9289	773, 753, 676, 434	0.9324
7	627	0.7510	840, 686	0.9184	928, 918, 618	0.9288	773, 753, 676, 637	0.9324
8	618	0.7472	773, 686	0.9184	928, 870, 686	0.9284	773, 753, 676, 540	0.9322
9	608	0.7042	763, 657	0.9182	928, 918, 608	0.9284	773, 753, 657, 521	0.9321
10	598	0.7018	966, 666	0.9182	928, 918, 647	0.9282	773, 753, 686, 521	0.9321
11	937	0.6670	763, 666	0.9182	773, 753, 618	0.9281	773, 753, 676, 502	0.9321
12	589	0.6619	850, 686	0.9182	928, 918, 657	0.9281	773, 763, 753, 676	0.9320
13	773	0.6611	870, 676	0.9181	928, 918, 666	0.9281	773, 753, 676, 560	0.9320
14	782	0.6609	763, 647	0.9181	773, 753, 666	0.9280	773, 753, 676, 666	0.9320
15	957	0.6607	763, 608	0.9181	773, 753, 627	0.9280	773, 753, 686, 637	0.9320
16	947	0.6569	870, 657	0.9180	928, 918, 637	0.9279	773, 753, 676, 443	0.9318
17	753	0.6557	831, 686	0.9179	928, 918, 627	0.9278	773, 763, 753, 686	0.9318
18	802	0.6554	918, 686	0.9178	928, 870, 676	0.9276	773, 753, 676, 579	0.9318
19	840	0.6540	918, 676	0.9178	928, 918, 598	0.9273	773, 753, 676, 550	0.9318
20	502	0.6536	966, 657	0.9177	928, 870, 618	0.9272	937, 773, 753, 676	0.9318

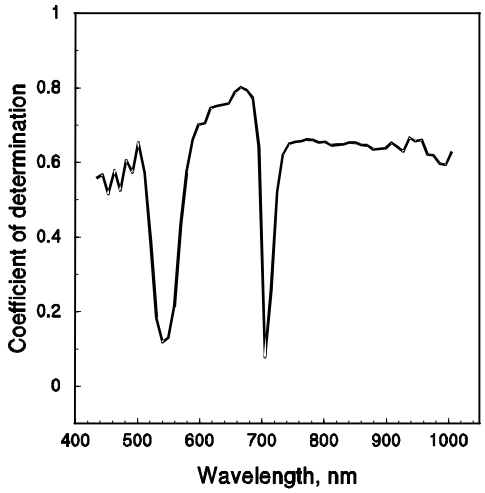

Figure 2. Coefficient of determination for percent canopy cover as a function of individual bands, for merged data from ten flights.

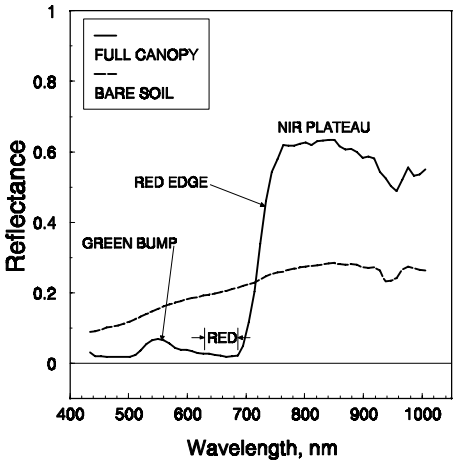

Figure 3. Spectral response patterns for bare soil where plants were removed from the east end of field 42 and for full canopy plants at the west end of field 41 on 1 July 2002.

Results and Discussion

Band Selection and Vegetation Indices

The percent canopy cover was found to be related to several different combinations of bands. The models with the 20 highest r^2 for one band, two bands, three bands, and four bands are given in table 2. As seen in figure 2, the r^2 for the single-band models in the red range (598 to 686 nm) are much higher than those in the NIR range (744 to 957 nm), suggesting that more weight should be given to the red bands. The 666 nm band is apparently much more important than the 686 nm band. There is a large range of NIR wavelengths all with about the same degree of correlation, $r^2 > 0.62$. At the 502 nm band, the r^2 is just as high as in the NIR range. The low r^2 value at 705 nm is close to the point where the spectral response patterns for bare soil and vegetation cross, as seen in figure 3, and so they have equal reflectance. The other low-correlation area is at the green bump, 531 to 560 nm.

The r^2 values for two-band models were generally very good, with all of the top 100 in the range of 0.9159 to 0.9192. In every case, one of the two terms was from the red range. In 99 out of 100 cases, the other term was from either the NIR plateau or the upper end of the red edge. The lone exception consisted of the bands at 598 and 531 nm, ranked 76th. The 966 nm band worked well in combination with any band between 618 and 686 nm. Increasing the number of parameters (bands) in the regression analysis generally increased the r^2 value, although much more so in going from one band to two bands than from two bands to three bands. Going from three bands to four bands provided little improvement. In every case in the top 20 of the three-band models, each of the terms shown in table 2 contributed significantly ($p < 0.001$) to the r^2 value. There was little difference in the value of r^2 for the top rank (0.9310) and the 100th rank (0.9228) for the three-band models. In 99 out of 100 cases, one of the three terms was from the red range, and the band that appeared most

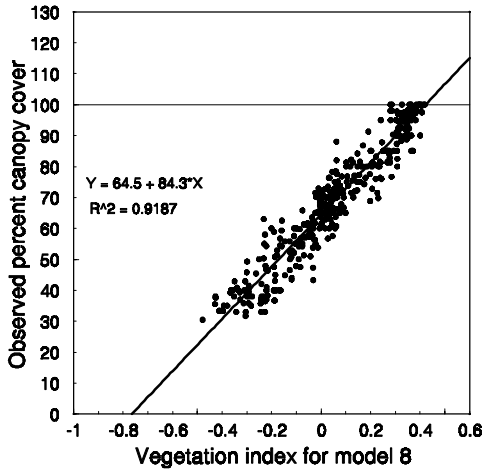

Figure 4. Scatter diagram for observed percent canopy cover vs. the two-band vegetation index for model 8 ($I = R_{966} - 5.273*R_{676}$). RMSE = 5.74%. R_{966} and R_{676} are the reflectances at 966 and 676 nm, respectively.

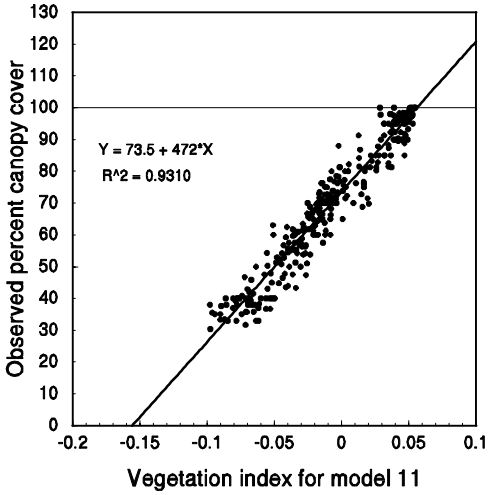

Figure 5.Scatter diagram for observed percent canopy cover vs. the three-band vegetation index for model 11 ($I = R_{773} - 0.937*R_{753} - 0.921*R_{676}$). RMSE = 5.29%.

Table 3. Regression equations for percent canopy cover models with the five highest r^2 in each category.

Model	Category (No. of Parameters)	Rank	Equation	r^2	RMSE (%)
1	1	1	$G = 108.3 - 619.9*R_{666}$	0.8023	8.94
2	1	2	$G = 107.5 - 603.9*R_{676}$	0.7947	9.12
3	1	3	$G = 111.0 - 645.2*R_{657}$	0.7888	9.25
4	1	4	$G = 110.9 - 607.8*R_{686}$	0.7731	9.59
5	1	5	$G = 113.9 - 670.6*R_{647}$	0.7583	9.89
6	2	1	$G = 71.1 + 55.3*(R_{763} - 7.74*R_{686})$	0.9192	5.72
7	2	2	$G = 64.7 + 89.4*(R_{966} - 4.96*R_{686})$	0.9189	5.73
8	2	3	$G = 64.5 + 84.3*(R_{966} - 5.27*R_{676})$	0.9187	5.74
9	2	4	$G = 73.8 + 57.5*(R_{763} - 8.43*R_{637})$	0.9186	5.74
10	2	5	$G = 68.4 + 67.5*(R_{870} - 6.41*R_{686})$	0.9185	5.74
11	3	1	$G = 73.5 + 472.2*(R_{773} - 0.937*R_{753} - 0.921*R_{676})$	0.9310	5.29
12	3	2	$G = 73.5 + 440.8*(R_{773} - 0.920*R_{753} - 0.978*R_{686})$	0.9305	5.30
13	3	3	$G = 75.0 + 441.7*(R_{773} - 0.926*R_{753} - 1.043*R_{657})$	0.9301	5.32
14	3	4	$G = 72.0 - 186.8*(R_{928} - 1.249*R_{918} + 2.396*R_{676})$	0.9290	5.36
15	3	5	$G = 74.5 + 435.1*(R_{773} - 0.914*R_{753} - 1.086*R_{647})$	0.9289	5.37
16	4	1	$G = 71.1 + 493.9*(R_{773} - 0.986*R_{753} - 1.245*R_{676} + 0.654*R_{531})$	0.9328	5.22
17	4	2	$G = 72.6 + 480.9*(R_{773} - 0.974*R_{753} - 1.320*R_{676} + 0.735*R_{521})$	0.9327	5.22
18	4	3	$G = 70.8 + 536.0*(R_{773} - 0.766*R_{753} - 0.799*R_{676} - 0.161*R_{811})$	0.9326	5.23
19	4	4	$G = 70.7 + 468.6*(R_{773} - 0.950*R_{753} - 1.619*R_{686} + 0.729*R_{695})$	0.9325	5.23
20	4	5	$G = 71.1 + 513.7*(R_{773} - 0.967*R_{753} - 1.365*R_{676} + 0.537*R_{695})$	0.9325	5.23

frequently was at 686 nm. The model with the highest r^2 in the three-band category contained 676, 753, and 773 nm, and these same terms showed up in the best four-band model. All 100 of the top four-band models included 753 nm and a red term, mostly 676 and 686 nm. In 95 out of 100 cases, 773 nm was also in the model. The range in r^2 values for the four-band category was 0.9310 to 0.9328. In the top 20, all four terms contributed significantly to the r^2 value.It is important to notice that there are many different combinations that work well. As suggested by Lillesand and Kiefer (1999), a unique solution would only be possible under ideal conditions.

Figure 4, which includes 300 points from ten flights, shows how well the data from one of the best two-band models (model 8 in table 3) fit the linear regression line. The *x*-axis for this plot was developed using equations 1, 2, and 3, and the regression line shown comes from equation 4. In this case, $a = 64.6$, $b = 84.3$, $c = 444.3$, $m = -5.273$, and the resulting $r^2 = 0.919$ and RMSE = 5.74%.

A similar vegetation index was developed for the three-parameter model, as shown in figure 5 and table 3. In this case, the three-parameter model had an r^2 of 0.931, which is considerably higher than for the two-parameter model. The root mean square error (RMSE) for the three-parameter model was 5.29%, which is much lower than the 5.72% for the two-parameter model. By comparing figures 4 and 5, one may note the difference in scatter around the regression lines. Table 3 shows the regression equations for the top five r^2 rankings in each category of model. The terms in parentheses are vegetation indices. For the three-parameter model, the bands at 753 and 773 nm occur in four out of the five top ranks. They have similar coefficients and opposite signs, indicating a possible importance of the slope of the spectral response pattern in that region, which is at the upper end of the

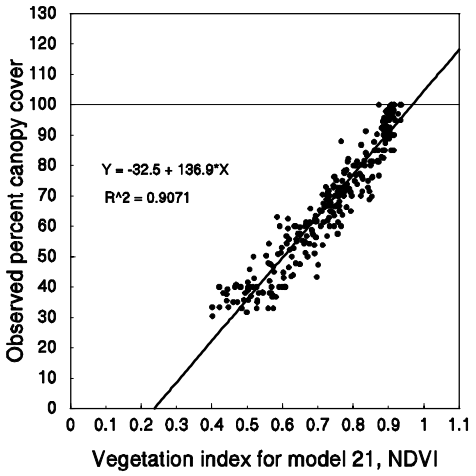

Figure 6. Scatter diagram for observed percent canopy cover vs. the vegetation index for model 21, *I* = NDVI = (Nir – Red) / (Nir + Red). RMSE = 6.13%.

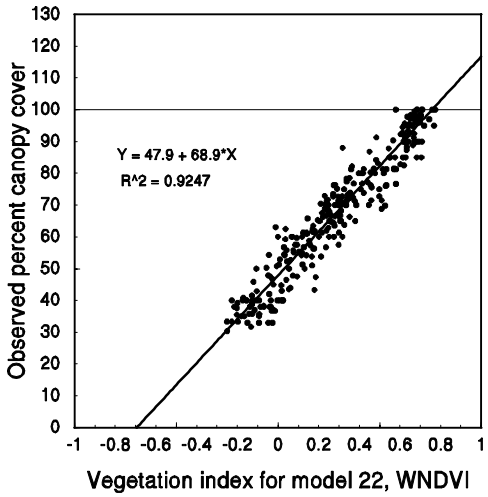

Figure 7. Scatter diagram for observed percent canopy cover vs. the vegetation index for model 22, *I* = WNDVI = (Nir – 3.9*Red) / (Nir + 3.9*Red). RMSE = 5.52%.

red edge. Likewise, in both tables 2 and 3, bands at 918 and 928 nm appear together several times, indicating that the slope in that region might also be important.

The normalized difference vegetation index (NDVI) is one of the oldest and most common vegetation indices used in remote sensing (Seidl et al., 2004) and is meant to be an indicator of crop cover and biomass: NDVI = (N–R)/(N+R), where N is NIR reflectance, and R is the red reflectance (Rouse et al., 1974; Vinogradov, 1977). In order to match the multispectral wavelengths used in the SAMRSS package, we used the average reflectance of 686 and 676 nm as the R value, and the average of 831 nm through 870 nm for the N value. Figure 6 is a scatter diagram showing how our observed values of percent canopy cover correspond to the NDVI. The linear fit is not quite as good as with the two-parameter model. One of the well-known problems with the NDVI is the saturation and insensitivity that occur at the higher levels of canopy cover (Mutanga and Skidmore, 2004; Carlson and Ripley, 1997).

Weighted NDVI

From the vegetation indices given for the two-band models in table 3, one notes that the first term is always in the NIR region (763 to 966 nm), and the coefficient on the red term (637 to 686 nm) is always much greater than unity, varying from 4.96 to 8.43. These are very high weighting factors. This suggests a modification in the NDVI, which normally has equal weighting on the NIR and red terms. Using the nonlinear regression program available in CoPlot, the observed percent canopy cover was regressed against the form (N – w*R)/(N + w*R), where w is a weighting factor. We call this form WNDVI, for weighted NDVI. The best correlation occurred with w = 3.9. Figure 7 shows how well this weighted NDVI corresponds to the observed percent canopy. The r^2 of 0.925 and RMSE of 5.52% make it a better fit than the two-parameter model, but not quite as good as the three-parameter model. Another model comes from the bands used in the NDVI (i.e., N – v*R), with the best correlation obtained with v = 8.034, and a resulting r^2 = 0.918 and RMSE = 5.76%. Table 4 shows the regression equations for percent canopy cover as a function of NDVI and for these new vegetation indices. All of the two-parameter models in table 2 were normalized and regressed to find the proper weighting factor, and the best three models are included in table 4 as models 25, 26, and 27. These three models are all narrow-band versions of the WNDVI. It appears that the best wavelengths to use with this weighted and normalized index are very close to those used with the NDVI.

Covariance

Using equation 4, the percent canopy cover was calculated for every line of HSI data in the averaged grid area file for the B and C plots of field 41 for the flight of 1 July 2002. The result was put in the 61st column. Likewise, the average scene temperature for each of these same grid areas was determined using the TIR data files, and the result was put in the 62nd column. These scene temperatures were then plotted against the average percent canopy cover in figure 8a. At that time, the B plots had only been deficit irrigated for five days and had not yet reached the threshold stress level.Naturally, the greater the canopy cover, the cooler the scene temperature, and analysis of covariance (Steele and Torrie, 1960) showed that there was indeed a very close linear relationship between the

Table 4. Regression equations for some additional vegetation indices.

Model	Vegetation Index (*I*)	Regression Equation	r^2	RMSE (%)
21	NDVI = (Nir – Red) / (Nir + Red)	G = –32.5 + 136.9 * I	0.9071	6.13
22	WNDVI = (Nir – 3.9Red) / (Nir + 3.9Red)	G = 47.9 + 68.9 * I	0.9247	5.52
23	Nir – 8.034Red	G = 70.6 + 53.7 * I	0.9180	5.76
24	WNDVI2 = (R_{966} – 3.3R_{676}) / (R_{966} + 3.3R_{676})	G = 47.7 + 71.4 * I	0.9182	5.76
25	(R_{850} – 3.96R_{686}) / (R_{850} + 3.96R_{686})	G = 48.4 + 69.9 * I	0.9255	5.49
26	(R_{840} – 4.03R_{686}) / (R_{840} + 4.03R_{686})	G = 48.7 + 70.0 * I	0.9252	5.50
27	(R_{831} – 3.94R_{686}) / (R_{831} + 3.94R_{686})	G = 48.3 + 69.7 * I	0.9254	5.50

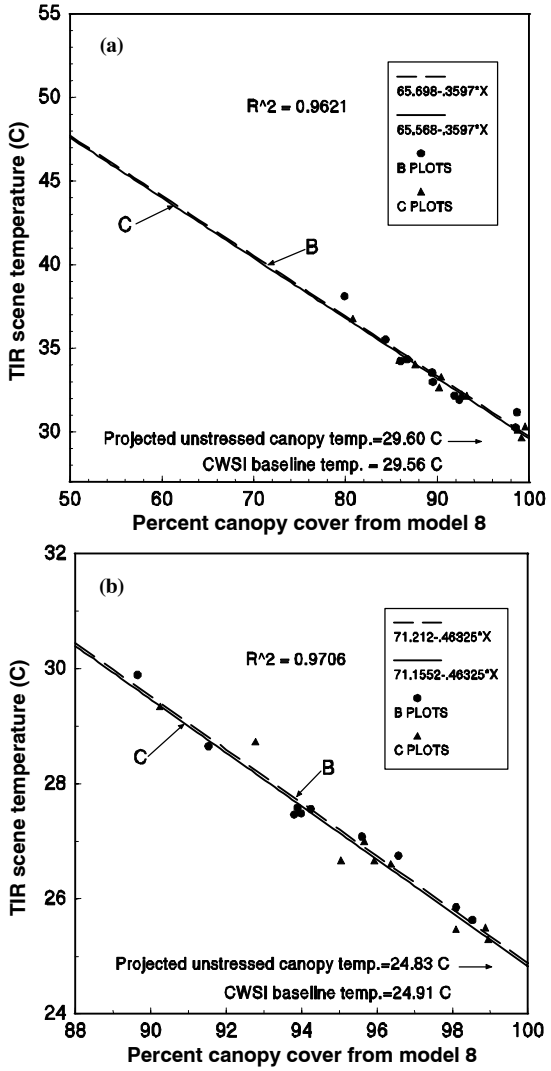

Figure 8. Scene temperature from TIR camera vs. percent canopy cover as calculated by model 8, $G = 64.5 + 84.3*(R_{966} - 5.273*R_{676})$, for field 41 on (a) 1 July 2002 and (b) 8 July 2002 before stress took effect in the B plots.

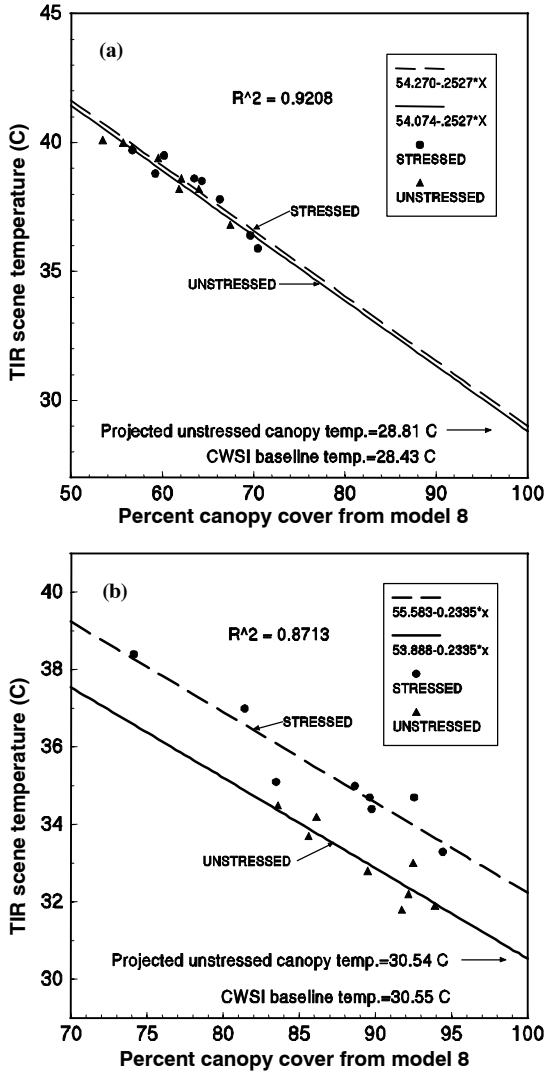

Figure 9. Scene temperature from TIR camera vs. percent canopy cover as calculated by model 8, $G = 64.5 + 84.3*(R_{966} - 5.273*R_{676})$, for field 21 on (a) 9 July 2003 before stress was applied and (b) 28 July 2003 after stress was applied to the stressed treatments. Irrigations were two weeks prior to flight.

two variables, with $r^2 = 0.962$. It also showed that there was no significant difference between the two treatments at the 5% level. The temperature difference between the two treatments, for the same percent canopy cover, was only 0.13°C, whereas the least significant difference (LSD_{05}) required was 0.47°C. When the temperature data were projected (adjusted) to values corresponding to 100% canopy cover, the result was the temperature of the canopy alone, separated from the soil-canopy mixture of temperatures. The canopy temperature of healthy, well-watered cotton plants is usually several degrees below air temperature, and dependent on the vapor pressure deficit (VPD) of the air above the canopy. The lower baseline for the crop water stress index (CWSI), from Idso et al. (1981), can be used to predict unstressed canopy temperatures. Pinter and Reginato (1982) developed a baseline for cotton in Arizona. A very similar baseline was developed by DeTar et al. (2006) in California, with the baseline temperature given as:

$$T_b = T_a + 0.597 - 1.779 * P \qquad (5)$$

where

T_b = unstressed CWSI baseline temperature (°C)
T_a = temperature of the air above the canopy (°C)
P = vapor pressure deficit (VPD) of the air (kPa).

When projected to 100% canopy cover, as shown in figure 8a, the average temperature of the canopy alone in the B and C plots was found to be very close to the theoretical CWSI baseline temperature of 29.56°C. The B plots were projected to be 29.73°C, and the C plots were projected to be 29.60°C. The regression equation for the C plots suggests that if the relationship were linear for the range of 0% to 75% canopy, there would be a virtual (apparent) temperature of 65.6°C for the bare soil, which is in the range of some of the soil temperatures actually measured at flight time. The r^2 of 0.962 indicated that over 96% of the variability in the scene temperature was due to the degree of ground cover, and with an LSD_{05} of 0.47°C, there was a strong indication that the canopy temperature was very uniform. Examples of the covariance procedure are shown for three additional flights in figures 8b, 9a, and 9b. Figure 8b shows that the procedure

Table 5. Comparison of eight canopy cover models used in covariance procedure for four flights: baseline error, r^2, and projection slope.

Measure	Model (name)	Bands (nm)	1 July 2002 Field 41	8 July 2002 Field 41	9 July 2003 Field 21	28 July 2003 Field 21	RMSE or Average
$T_{cu} - T_b$[a]	8	966, 676	0.04	−0.08	0.38	−0.01	0.195
	7	966, 686	0.55	0.26	0.47	−0.04	0.384
	6	763, 686	−1.49	−0.43	0.30	0.16	0.794
	11	773, 753, 676	0.00	−0.57	0.51	0.38	0.427
	21 (NDVI)	Nir, Red	−1.57	−0.89	2.84	−1.40	1.822
	22 (WNDVI)	Nir, Red	0.64	2.45	1.93	−0.01	1.592
	24 (WNDVI2)	966, 676	2.09	3.13	2.19	0.02	2.177
	23 (Nir – 8Red)	Nir, Red	−1.50	−0.42	0.23	0.28	0.608
r^2	8	966, 676	0.9621	0.9706	0.9208	0.8713	0.9312
	7	966, 686	0.9623	0.9712	0.9154	0.8875	0.9341
	6	763, 686	0.9613	0.9612	0.9403	0.9014	0.9411
	11	773, 753, 676	0.9441	0.8953	0.9673	0.8959	0.9257
	21 (NDVI)	Nir, Red	0.9729	0.9783	0.9254	0.8477	0.9311
	22 (WNDVI)	Nir, Red	0.9675	0.9783	0.9406	0.8416	0.9320
	24 (WNDVI2)	966, 676	0.9686	0.9773	0.9334	0.8100	0.9222
	23 (Nir – 8Red)	Nir, Red	0.9612	0.9573	0.9374	0.8945	0.9376
S_t[b]	8	966, 676	−0.360	−0.463	−0.253	−0.234	
	7	966, 686	−0.349	−0.456	−0.243	−0.227	
	6	763, 686	−0.370	−0.482	−0.254	−0.228	
	11	773, 753, 676	−0.290	−0.441	−0.244	−0.190	
	21 (NDVI)	Nir, Red	−0.460	−0.671	−0.192	−0.329	
	22 (WNDVI)	Nir, Red	−0.317	−0.414	−0.203	−0.241	
	24 (WNDVI2)	966, 676	−0.345	−0.373	−0.199	−0.217	
	23 (Nir – 8Red)	Nir, Red	−0.418	−0.455	−0.25	−0.224	

[a] $T_{cu} - T_b$ = error in the baseline temperature, where T_{cu} is the projected canopy temperature (°C) for the unstressed treatments.
[b] S_t = slope of the regression equations found with analysis of covariance for mean grid−area temperature as a function of the mean value of the calculated percent canopy cover.

continued to show no difference in the treatment a week later, when the stress still had not taken effect in the B plot of field 41. It also shows again the very high degree of uniformity in the canopy temperature, with an r^2 of 0.971 and an LSD_{05} of 0.23°C. Figures 9a and 9b show the covariance relationship before and after the stress treatment was applied to field 21 in 2003, with good uniformity of canopy temperature on 9 July 2003 (r^2 = 0.921, LSD_{05} = 0.42°C) and a little more variability on 28 July 2003 (r^2 = 0.871, LSD_{05} = 0.48°C).

Some of the models for percent canopy cover worked better than others in this procedure. Tables 5 and 6 show how eight of the models compare by six different measures of performance for four flights. Of critical importance is how well the canopy temperature was predicted. The difference between the predicted unstressed canopy temperature and the CWSI baseline temperature is shown first, with models 7, 8, and 11 having the lowest average (RMSE) differences; they had no differences greater than 0.57°C. All the other models had differences of at least 1.49°C on one flight or another. The r^2 values showed little difference overall, but model 11 had an unusually low value on the flight of 8 July 2002. The slope (S_t), which is very important in the projection procedure, can vary considerably from one model to another, and between flights for the same model, but the slope for model 21 (NDVI) is unusually high, as compared to the other models, for three of four flights. The apparent soil temperature (*y*-intercept) for model 21 also shows up extremely high for one of the flights, at 91.3°C. The predicted temperature difference between the stressed and unstressed treatments are all small (≤0.28°C) for the first three flights, as it should be since stress had not yet been applied. NDVI is known to have problems with saturation at the upper end of the range of canopy cover (90% to 100%), and that may introduce a shortened range on the values for the vegetation index and the predicted percent canopy cover, which in turn causes the greater slope and higher intercept. In spite of this problem, the NDVI model still did well in predicting differences in canopy temperature; however, it did not do well in predicting the unstressed baseline temperature. After the stress was applied, differences varied from 1.51°C to 1.78°C for seven of the eight models; however, model 11 had a difference of 1.97°C, which made it an outlier two standard deviations above the average.

The F-test results in table 6 show that none of the temperature differences were significant at the 5% level for the first three flights, but they were all significant on the fourth flight. This means that the covariance procedure, for all eight models, did indeed indicate significant water stress when there was supposed to be, and it also showed that there was no water stress before the treatment was applied. By all the measures, models 7 and 8 had the fewest anomalies, and model 8 (two-band, using 966 and 676 nm) was chosen for the example because it came closest to predicting the CWSI baseline temperature.

As further confirmation of the procedure for predicting differences in canopy temperatures, the hand-held infrared thermometer was used on small areas just west of the walkways for all plots in field 21 during a 40 min time period close to the flight time on 28 July 2003. The stressed plots averaged 31.35°C and the unstressed plots 29.77°C, for a difference of 1.58°C. The least significant difference, at 5%, was 1.41°C. Leaf water potential, measured four days before the flight, averaged −1.49 MPa for the unstressed plots and

Table 6. Comparison of eight canopy cover models used in covariance procedure for four flights: soil temperature, treatment temperature difference, and F-test.

Measure	Model (name)	Bands (nm)	1 July 2002 Field 41	8 July 2002 Field 41	9 July 2003 Field 21	28 July 2003 Field 21
Y_0[a]	8	966, 676	65.6	71.2	54.1	53.9
	7	966, 686	65.0	70.7	53.7	53.2
	6	763, 686	65.1	72.6	54.2	53.5
	11	773, 753, 676	58.6	68.4	53.3	49.9
	21 (NDVI)	Nir, Red	74.0	91.3	50.4	62.0
	22 (WNDVI)	Nir, Red	61.9	69.0	50.6	54.7
	24 (WNDVI2)	966, 676	66.2	65.4	50.5	52.3
	23 (Nir – 8Red)	Nir, Red	69.9	70.0	54.4	53.2
$T_{cs} - T_{cu}$[b]	8	966, 676	0.13	0.06	0.19	1.70
	7	966, 686	0.16	0.07	0.21	1.78
	6	763, 686	0.15	0.04	0.27	1.72
	11	773, 753, 676	0.27	0.10	0.21	1.97
	21 (NDVI)	Nir, Red	0.19	0.21	0.28	1.55
	22 (WNDVI)	Nir, Red	0.18	0.21	0.28	1.56
	24 (WNDVI2)	966, 676	0.19	0.22	0.21	1.51
	23 (Nir – 8Red)	Nir, Red	0.15	0.07	0.25	1.70
F-test[c]	8	966, 676	0.31	0.08	0.86	45.4
	7	966, 686	0.52	0.30	0.93	58.7
	6	763, 686	0.42	0.13	2.22	61.5
	11	773, 753, 676	1.14	0.16	2.27	77.3
	21 (NDVI)	Nir, Red	1.15	4.14	1.77	30.4
	22 (WNDVI)	Nir, Red	0.83	3.85	2.51	29.7
	24 (WNDVI2)	966, 676	0.78	4.40	1.22	22.8
	23 (Nir – 8Red)	Nir, Red	0.28	0.21	1.80	53.7

[a] Y_0 is the y-intercept for the unstressed regression equation and the apparent temperature (°C) for bare soil.
[b] $T_{cs} - T_{cu}$ is the temperature difference between stressed and unstressed treatments.
[c] For a significant difference between stressed and unstressed treatments, $F_{05} \geq 4.45$.

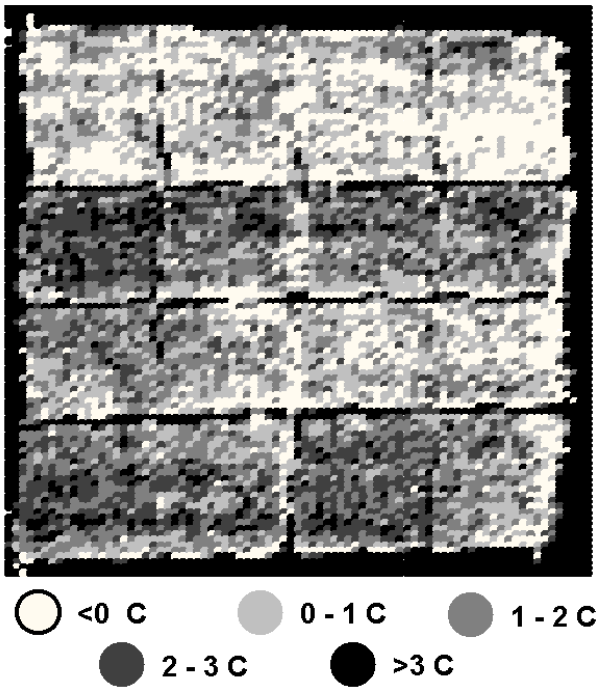

Figure 10. High-definition stress image (HDSI) of field 21 on 28 July 2003, showing the temperature rise above the CWSI baseline, in ˚C, with 1.0 m spatial resolution.

−1.76 MPa for the stressed plots. The critical level for scheduling an irrigation of cotton at this stage of growth is given by Hake et al. (1996) as −1.8 MPa.

High-Definition Stress Image (HDSI)

The image map in figure 10, which is for the flight of 28 July 2003 over field 21, was developed by the following procedure. First, every point in figure 9b was projected to the value it would have had at 100% canopy cover, using the following equation:

$$T_c = T_g + S_t * (100 - G) \quad (6)$$

where

T_g = average TIR temperature for the grid area (˚C)
T_c = adjusted TIR temperature (˚C)
S_t = slope of the covariance regression lines, which in this case was −0.2335.

The adjusted TIR value (T_c), which is also the canopy temperature, was then added to the averaged grid-area data files as column 63. The green-red vegetation index (GRVI), which is the difference in reflectance of the green (550 nm) and red (average of 676 and 686 nm) bands, was found by analysis of covariance to be closely related to stress and percent canopy cover, as seen in figure 11. The GRVI was adjusted to 100% canopy cover in a manner similar to that for TIR, using an equation similar to equation 6:

$$I_{ga} = I_g + S_g * (100 - G) \quad (7)$$

where

I_g = GRVI
I_{ga} = adjusted GRVI
S_g = slope of the covariance regression lines, which in this case was 0.001201.

The GRVI and the adjusted GRVI were added to the averaged grid area data file as columns 64 and 65, respectively.

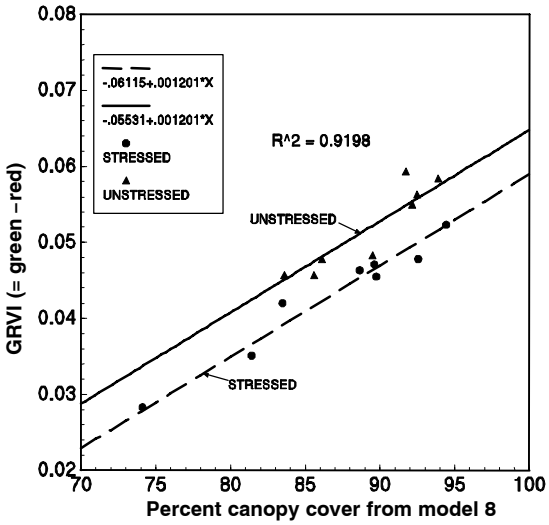

Figure 11. GRVI (green minus red) vs. percent canopy cover as calculated by model 8, G = 64.5 + 84.3*(R_{966} − 5.273*R_{676}), for field 21 on 28 July 2003 (r^2 = 0.9198 and LSD_{05} = 0.0023).

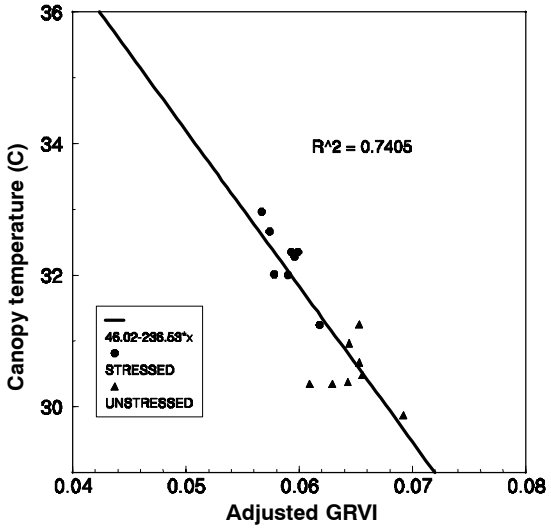

Figure 12. Canopy temperature (adj. TIR) vs. adjusted GRVI for field 21 on 28 July 2003.

T_c was then regressed on I_{ga}, with the resulting equation:

$$T_c = 46.02 - 236.5 * I_{ga} \quad (8)$$

r^2 = 0.741 and RMSE = 0.18°C

This relationship is also shown in figure 12.

Next, using equation 4, the percent canopy (G) was calculated for every pixel in the ROI data file (over 8300 rows of data in Excel) for field 21. Columns were added for GRVI and the adjusted GRVI. Using equation 8, T_c was calculated for every pixel. The CWSI baseline canopy temperature (T_b from eq. 5) of 30.55°C was then subtracted from the T_c values to produce the temperature rise (T_r), which was plotted using ArcView. It was noticed in the image that areas of bare soil around the outside edge of the field had unusually low temperatures. This was caused by the negative values for canopy cover when I in equation 4 was less than −0.76. To make these temperatures more realistic, a nonlinear equation was fitted to the data in figure 4, so that the function is asymptotic to the x-axis:

$$G_n = \left(1 - \left[1 - e\text{^}\left(-0.9255 + 1.879 * I\right)\right]\text{^}2\right) * 100 \quad (9)$$

This equation has an r^2 = 0.920 and RMSE = 5.66%, which are improvements over the values for the linear function. The plot in figure 10 was made with G_n substituted for G in the ROI data file.

Since plant water stress is proportional to the temperature rise (Jackson et al., 1981), the plot in figure 10 is an image map of the degree of stress at every part of the field, with a fairly sharp image, the spatial resolution being about 1.0 m. The darker areas of the image represent higher stress. Reginato (1983) suggested that a CWSI range of 0.2 to 0.3 was optimum for scheduling irrigation of cotton. This range corresponds to a temperature rise of 2°C to 3°C above the baseline for typical VPD values for this region, and according to Howell et al. (1984), it also corresponds to leaf water potentials of −1.7 to −1.8 MPa. So the white and light gray areas in figure 10 are not stressed. The medium gray areas could be considered marginal, while the dark gray and black areas are definitely water stressed.

To further verify the image map values, ArcView was used again to get the average canopy temperature in each grid area. The average canopy temperature was 30.88°C for the unstressed plots and 32.38°C for the unstressed plots, for a difference of 1.50°C, which is very close to that found by the hand-held infrared thermometer. More validation was obtained by looking at data for three flights over field 41A, which occurred on 25 June 2002, 1 July 2002, and 28 July 2003. These results are plotted in figure 13, showing an excellent fit, with an r^2 of 0.932 and an RMSE of 5.43%, when the obvious outlier is excluded. The outlier may be the result of some sort of edge effect, since it is in a plot at the western edge of the field.

Since some vegetation indices (VI) are sensitive to nitrogen levels in the plants, the five levels of nitrogen application were regressed on the VI for model 8 (R_{966} − 5.273*R_{676}) for field 21 on the flight of 28 July 2003, resulting in an r^2 of 0.0013. Similarly, for the VI for model 11 (R_{773} − 0.937*R_{753} − 0.921*R_{676}), the r^2 was 0.0033. So nitrogen detection was not a problem.

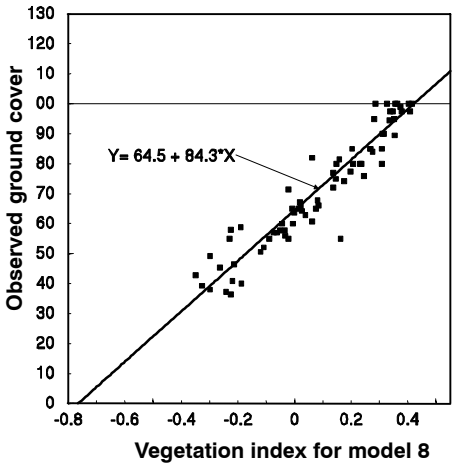

Figure 13. Scatter diagram for observed percent canopy cover vs. the vegetation index for model 8 (I = R_{966} − 5.273*R_{676}) for three validation flights over field 41A. The function shown is from the regression of the data used in figure 4.

Goel et al. (2003), looking at several bio-physical properties of corn, used multiple regression for band selection, as was done here. They were concerned that collinearity or co-dependence of the many band reflectances could be a problem, as suggested by Longley (1967) and Beaton et al. (1976). However, with the goal of prediction rather than explanation, collinearity is less of a problem (Yu, 2000; Haan, 1977). CoPlot has a diagnostic tool that automatically checks for collinearity using a procedure from Maindonald (1984). Band selection using multiple regression was also used successfully by DeTar et al. (2006). Multiple regression is a simple and straightforward method for obtaining optimum bands, and the resulting vegetation indices worked well over a wide variety of field and atmospheric conditions.

Conclusions

The main result this study shows is that under the conditions of partial canopy in cotton over a dry soil surface, there are several new vegetation indices (VIs) that are better than NDVI at predicting percent canopy cover. One is a weighted NDVI, where a coefficient of 3.9 is applied to the red term; using this should make calibration less of a problem than with the normal NDVI. With the goal of showing the difference in stress in some experimental irrigation treatments, a covariance projection procedure was presented for separating the canopy temperature from the scene temperature. Some of the new VIs work better than others with this procedure, among which is a two-parameter model using the reflectance at wavelengths of 676 and 966 nm. The canopy in the stressed treatment of one experiment was shown to have a significantly higher temperature than in an unstressed treatment. Analysis of covariance showed that the vegetation index GRVI (the difference between the reflectance of the green and red wavelengths) was closely related to both percent canopy cover and water stress. Using GRVI, TIR, and new models for percent canopy cover, it was possible to create a high-definition stress image showing the degree of plant water stress in every part of a cotton field.

The information presented here should be useful in selecting filters for multispectral cameras and for selecting wavebands for HSI cameras when attempting to measure degree of ground cover. A straightforward method was presented for separating canopy temperature from soil temperature, and a procedure was given for producing a detailed map of canopy temperatures so that small hot spots can be detected before they become large hot spots.

Acknowledgements

The authors wish to thank H. A. Funk for taking care of the field plots and collecting data. They also appreciate the work of the farm crew of the UC Shafter Research and Extension Center. Special thanks goes to the five reviewers who contributed many good ideas to the manuscript.

References

Allen, R. G., L. S. Pereira, D. Raes, and M. Smith. 1998. Crop evapotranspiration guidelines for computing crop water requirements. Irrigation and Drainage Paper 56. Rome, Italy: United Nations FAO.

Bajwa, S. G., P. Bajcsy, P. Groves, and L. F. Tian. 2004. Hyperspectral image data mining for band selection in agricultural applications. *Trans. ASAE* 47(3): 895-907.

Beaton, A. E., D. B. Rubin, and J. L. Barone. 1976. The acceptability of regression solutions: Another look at computational accuracy. *J. American Stat. Assoc*. 71(353): 158-168.

Carlson, T. N., and D. A. Ripley. 1997. On the relation between NDVI, fractional vegetation cover, and leaf area index. *Remote Sens. Environ.* 62(3): 241-252.

Clarke. T. R. 1997. An empirical approach for detecting crop water stress using multispectral airborne sensors. *Hort. Tech*. 7(1): 9-16.

Dawson, C. J. 1997. Management of spatial variability. In *Precision Agriculture '97: Vol. I. Spatial Variability in Soil and Crop*, 45-58. J. V. Stafford, ed. Oxford, U.K.: BIOS Scientific Publishers.

DeTar, W. R. 2004. Using a subsurface drip irrigation system to measure crop water use. *Irrig. Sci.* 23(3): 111-122.

DeTar, W. R., J. V. Penner, and H. A. Funk. 2006. Airborne remote sensing to detect plant water stress in full canopy cotton. *Trans. ASABE* 49(3): 655-665.

Ehrler, W. L., S. B. Idso, R. D. Jackson, and R. J. Reginato. 1978. Wheat canopy temperature: Relation to plant water potential. *Agron. J*. 70(2): 251-256.

Goel, P. K., S. O. Prasher, J. A. Landry, R. M. Patel, A. A. Viau, and J. R. Miller. 2003. Estimation of crop biophysical parameters through airborne and field hyperspectral remote sensing. *Trans. ASAE* 46(4): 1235-1246.

Haan, C. T. 1977. *Statistical Methods in Hydrology.* Ames, Iowa: Iowa State University Press.

Hake, S. J., D. W. Grimes, K. D. Hake, T. A. Kerby, D. J. Munier, and L. J. Zelinski. 1996. Irrigation scheduling. In *Cotton Production Manual*, 228-247. Publication 3352. Oakland, Cal.: University of California, Division of Agricultural and Natural Resources.

Howell, T. A., J. L. Hatfield, H. Yamada, and K. R. Davis. 1984. Evaluation of cotton canopy temperature to detect crop water stress. *Trans. ASAE* 27(1): 84-88.

Idso, S. B., R. D. Jackson, P. J. Pinter, Jr., R. J. Reginato, and J. L. Hatfield. 1981. Normalizing the stress-degree-day parameter for environmental variability. *Agric. Meteorol.* 24: 45-55.

Jackson, R. D., S. B. Idso, R. J. Reginato, and P. J. Pinter, Jr. 1981. Canopy temperature as a crop stress indicator. *Water Resources Res.* 17(4): 1133-1138.

Jackson, R. D., P. N. Slater, and P. J. Pinter, Jr. 1983. Discrimination of growth and water stress in wheat by various vegetation indices through clear and turbid atmospheres. *Remote Sens. Environ.* 13(3): 187-208.

Lillesand, T. M., and R. W. Kiefer. 1999. *Remote Sensing and Image Interpretation.* 4th ed. New York, N.Y.: John Wiley and Sons.

Longley, J. W. 1967. An appraisal of least squares procedures for the electronic computer from the point of view of the user. *J. American Stat. Assoc.* 62(319): 819-841.

Maas, S. J. 1998. Estimating cotton canopy ground cover from remotely sensed scene reflectance. *Agron. J.* 90(3): 384-388.

Maas, S. J., G. J. Fitzgerald, W. R. DeTar, and P. J. Pinter, Jr. 1999. Detection of water stress in cotton using multispectral remote sensing. In *Proc. Beltwide Cotton Conf.*, 2: 584-585. Memphis, Tenn.: National Cotton Council.

Maindonald, J. H. 1984. *Statistical Computation.* New York, N.Y.: John Wiley and Sons.

Moran, M. S., P. J. Pinter, Jr., B. E. Clothier, and S. G. Allen. 1989. Effect of water stress on the canopy architecture and spectral indices of irrigated alfalfa. *Remote Sens. Environ.* 29(3): 251-261.

Moran, M. S., T. R. Clarke, Y. Inoue, and A. Vidal. 1994. Estimating crop water deficit using the relation between surface-air tem-

perature and spectral vegetation index. *Remote Sens. Environ*. 49(3): 246-263.
Moran, M. S., Y. Inoue, and E. M. Barnes. 1997. Opportunities and limitations for image-based remote sensing in precision crop management. *Remote Sens. Environ*. 61(3): 319-346.
Mutanga, O., and A. K. Skidmore. 2004. Narrow-band vegetation indices overcome the saturation problem in biomass estimation. *Intl. J. Remote Sens.* 25(19): 3999-4014.
Pinter, P. J., Jr., and R. J. Reginato. 1982. A thermal infrared technique for monitoring cotton water stress and scheduling irrigations. *Trans. ASAE* 25(6): 1651-1655.
Reginato, R. J. 1983. Field quantification of crop water stress. *Trans. ASAE* 26(3): 772-775, 781.
Rouse, J. W., R. H. Haas, J. A. Schell, D. W. Deering, and J. C. Harlan. 1974. Monitoring the vernal advancement and retrogradation (greenwave effect) of natural vegetation. Type III. Final report. Greenbelt, Md.: NASA Goddard Space Flight Center.
Seidl, M. S., W. D. Batchelor, and J. O. Paz. 2004. Integrating remotely sensed images with a soybean model to improve spatial yield simulation. *Trans. ASAE.* 47(6): 2081-2090.
Steel, R. G. D., and J. H. Torrie. 1960. *Principles and Procedures of Statistics.* New York, N.Y.: McGraw-Hill.
Thenkabail, P. S., R. B. Smith, and E. DePauw. 2000. Hyperspectral vegetation indices and their relationships with agricultural crop characteristics. *Remote Sens. Environ.* 71(2): 158-182.
Thorp, K. R., L. Tian, H. Yao, and L. Tang. 2004. Narrow-band and derivative-based vegetation indices for hyperspectral data. *Trans. ASAE* 47(1): 291-299.
Vinogradov, B. V. 1977. Remote sensing in ecological botany. *Remote Sens. Environ.* 6(2): 83-94.
Wanjura, D. F., and D. R. Upchurch. 2000. Canopy temperature characterizations of corn and cotton water status. *Trans. ASAE* 43(4): 867-875.
Wiegand, C. L., A. J. Richardson, D. E. Escobar, and A. H. Gerbermann. 1991. Vegetation indices in crop assessments. *Remote Sens. Environ.* 35(2-3): 105-119.
Yu, C. H. 2000. An overview of remedial tools for collinearity in SAS. In *Proc. 2000 Western Users of SAS Software Conference*, 196-201. Scottsdale, Ariz.: Western Users of SAS Software, Inc.